Symmetry-adapted-cluster/symmetry-adapted-cluster configuration interaction methodology extended to giant molecular systems: Ring molecular crystals

Hiroshi Nakatsuji,[a] Tomoo Miyahara, and Ryoichi Fukuda
Department of Synthetic Chemistry and Biological Chemistry, Graduate School of Engineering,
Kyoto University, Katsura, Nishikyo-ku, Kyoto 615-8510, Japan and Quantum Chemistry Research Institute,
58-8 Mikawa, Momoyama-cho, Fushimi-ku, Kyoto 612-8029, Japan

The symmetry adapted cluster (SAC)/symmetry adapted cluster configuration interaction (SAC-CI) methodology for the ground, excited, ionized, and electron-attached states of molecules was extended to giant molecular systems. The size extensivity of energy and the size intensivity of excitation energy are very important for doing quantitative chemical studies of giant molecular systems and are designed to be satisfied in the present giant SAC/SAC-CI method. The first extension was made to giant molecular crystals composed of the same molecular species. The reference wave function was defined by introducing monomer-localized canonical molecular orbitals (ml-CMO's), which were obtained from the Hartree-Fock orbitals of a tetramer or a larger oligomer within the electrostatic field of the other part of the crystal. In the SAC/SAC-CI calculations, all the necessary integrals were obtained after the integral transformation with the ml-CMO's of the neighboring dimer. Only singles and doubles excitations within each neighboring dimer were considered as linked operators, and perturbation selection was done to choose only important operators. Almost all the important unlinked terms generated from the selected linked operators were included: the unlinked terms are important for keeping size extensivity and size intensivity. Some test calculations were carried out for the ring crystals of up to 10 000-mer, confirming the size extensivity and size intensivity of the calculated results and the efficiency of the giant method in comparison with the standard method available in GAUSSIAN 03. Then, the method was applied to the ring crystals of ethylene and water 50-mers, and formaldehyde 50-, 100-, and 500-mers. The potential energy curves of the ground state and the polarization and electron-transfer-type excited states were calculated for the intermonomer distances of 2.8–100 Å. Several interesting behaviors were reported, showing the potentiality of the present giant SAC/SAC-CI method for molecular engineering. © *2007 American Institute of Physics.*
[DOI: 10.1063/1.2464113]

I. INTRODUCTION

The recent trend in theoretical chemistry is threefold: more and more accurate predictions, larger and larger system applicability, and variety-of-states applicability.[1] Since the Schrödinger equation and its relativistic counterpart, Dirac-Coulomb equation, for example, are the basic principles governing chemistry,[2] the most straightforward way of achieving the first purpose of theoretical chemistry is to construct a general method of solving the Schrödinger and Dirac-Coulomb equations as accurately as possible. Recently, we could pave a way for this approach: we have proposed a general method of solving the Schrödinger equation in an analytical expansion form and extended this method for solving the Dirac-Coulomb equation of many-electron systems.[3,4] So far, the applications are limited only to very small atoms and molecules. We are now developing the methodology for making it applicable to larger molecular systems; however, some times are necessary for accomplishing this purpose for really large chemical systems.

Chemistry deals with a variety of systems. Among others, many interesting topics are related to giant molecular systems that cannot be handled in a reliable manner with the existing electronic structure theories. In chemistry, the theory must be in kcal/mol accuracy, at least, for being quantitatively predictive. Semiempirical methods are not reliable enough quantitatively and we have to use *ab initio* methodology. The Hartree-Fock theory does not have such an accuracy and the theory must include electron correlations. For dealing with giant molecular systems, the theory must satisfy the size extensivity for energy and the size intensivity for properties. An extensive property scales with the size of the system and an intensive property is independent of the size of the system.[5] Otherwise, the size-extensivity error in energy may easily reach an order of few rydbergs, which is by far larger than the chemical accuracy.

Chemistry involves not only the ground electronic states of molecules, but also various kinds of excited and ionized states. It is desirable if the theory can deal with both ground and excited states at the same time in the same accuracy. Generally speaking, the excitation and ionization energies

[a]Electronic mail: hiroshi@sbchem.kyoto-u.ac.jp

126, 084104-1

become smaller as the size of the system increases. There are many photoelectron processes that are really important in biology,[6] such as photosynthesis,[7] visions,[8] etc., and in molecular engineering.[9] We have to develop the methodology that is able to handle these photoelectron processes in large and giant molecular systems.

Among the theories including electron correlations, only few theories satisfy these requirements, namely, the size-extensivity requirement and the variety-of-states applicability. Among others, the symmetry adapted cluster[10] (SAC) and SAC configuration interaction[11] (SAC-CI) methodology developed in our laboratory[12,13] satisfies these requirements. In principle, the SAC/SAC-CI method can give the accuracy of kcal/mol, is size extensive and size intensive, and can deal with many different electronic states in a similar reliable accuracy. So, we want to extend here the SAC/SAC-CI methodology to giant molecular systems. The standard version of the SAC/SAC-CI program is incorporated in the GAUSSIAN 03 program.[12,14] With this program, we first calculate the singlet closed-shell (ground) state of a molecule by the SAC method and then calculate, with the SAC-CI method, the singlet excited states, triplet ground and excited states, and doublet ionized and/or electron-attached ground and excited states. One can further calculate quartet-to-septet ground and excited states generated from the SAC ground states. For the excited states involving more than two electron excitation and/or ionization processes, the SAC-CI general-R method[11] is more accurate than the ordinary single double (SD) R method. The energy gradients, which are the forces acting on the constituent nuclei, can be calculated for any of the singlet-to-septet ground and excited states in both SD-R and general-R methods.[15] Thus, we can study a variety of chemistry and physics with the SAC/SAC-CI methodology, ranging from fine spectroscopy of small molecules[12,13,16,17] to photobiological phenomena[18,19] involving relatively large molecules. Since we have a lot of experiences about this methodology, and we know that this method is certainly very useful for studying chemistries involving many different electronic states, we want to extend this methodology to giant molecular systems. This would enable seamless applications of this methodology from very fine spectroscopy to biological and nanomaterial chemistry. This paper is the first paper of this series of studies and will describe an extension of the SAC/SAC-CI method to weakly interacting molecular systems such as molecular crystal.

Several *ab initio* quantum chemistry approaches have been published for dealing with large and giant molecular systems. Imamura and co-workers reported an elongation method[20,21] which is suitable for the study of polymers. Förner *et al.*[22] reported a coupled cluster theory for applications to polymers. Kitaura and co-workers[23] reported a fragment molecular orbital method and applied this extensively to giant molecular systems: this method gives primarily energetic quantities but does not seem to give the corresponding wave functions. Sato *et al.*[24] developed a density functional code for calculations of proteins. The so-called linear-scaling methods have also been developed with different theories and in different levels of approximations.[25,26] These methods would have general utilities for the studies of large

molecular systems. Yang[27] developed a divide-and-conquer method in density functional theory. Scuseria[28] reported a linear-scaling density functional method. Werner and co-workers[29,30] developed linear-scaling electron correlation methods, in particular, coupled cluster method. Head-Gordon and co-workers[31] also reported linear-scaling algorithms for electronic structure methods. Nakajima and co-workers[32] published several fast algorithms in electronic structure calculations. In many of the above treatments, localized orbitals were used to efficiently describe the correlation effects in the ground state. For excited states, however, a canonical picture is often useful but contradicts the localized picture.

In the next section, we describe our basic idea for extending the SAC/SAC-CI methodology to giant molecular systems. We consider in this paper the extension of the SAC/SAC-CI methodology to cyclic molecular crystal composed of a single molecular species *A*. We choose cyclic molecular crystals as first applications of the giant SAC/SAC-CI methodology because we have to check the accuracy of the giant methodology in comparison with the standard version of the SAC-CI program. For ring systems, we can change the size freely, so that for small systems we can perform both giant and standard SAC/SAC-CI calculations, compare directly their results, and see the accuracy of the giant version. For three-dimensional crystals, we cannot do such direct comparisons because the standard calculations are impossible to perform for infinite systems. After confirming that the basic approximations in the giant SAC/SAC-CI methodology are acceptable, it is a straightforward matter to extend the present algorithms to three-dimensional molecular crystals.

We first define the reference wave function and orbitals for the SAC/SAC-CI calculations. To obtain both of the local picture and the canonical-orbital picture that are necessary for describing both ground and excited states, we introduce monomer-localized canonical molecular orbitals (ml-CMO's) of the crystal. Using these reference orbitals and wave function, we then formulate the giant SAC method for the ground state and the giant SAC-CI method for the excited states. The structures of the linked and unlinked matrix elements are clarified. We account the details of the integral evaluations and the merits of the present method. Then, the method is applied to a number of systems. First, we check the nature of the ml-CMO's and the accuracy of the reference wave function in comparison with the Hartree-Fock wave function of the crystal. We also compare the results of the present giant SAC/SAC-CI with those of the standard SAC/SAC-CI incorporated in GAUSSIAN 03.[14] Next, we check that the present method satisfies the size extensivity of the calculated energy and the size intensivity of the excitation energy. Then, we calculate the potential energy curves of the ground and excited states of the C_2H_4, H_2O, and H_2CO ring crystals. Some interesting properties of these ring crystals are described. The conclusion of the present study is given in the last section. The extensions of the present methodology to three-dimensional molecular crystals, polymers, biological systems, etc., will be given in the succeeding papers.

We note here that the ground-state energy alone of the giant molecular crystal can be calculated rather easily both at the Hartree-Fock level and the correlation level by the ex-

trapolation method by assuming that the N-body interaction term becomes zero as N increases, though this method may not have much significance in chemistry because it does not give the corresponding wave function.

II. BACKGROUND OF THE GIANT SAC/SAC-CI METHOD

First, let us consider how experimentalists synthesize molecular crystals having interesting electronic properties. They gather isolated molecules in some technical way, arrange them utilizing the intermolecular forces in some specific way, and obtain molecular crystals,[33] which often show some interesting properties not expected from their isolated states. Such interesting properties sometimes come out when external fields, such as photon field, electric field, magnetic field, etc, are applied. We want to study underlying physical and chemical principles governing these phenomena.

A straightforward way for the theoretical chemists to simulate the above procedure of the experimental chemists would be to write down the wave function of the molecular crystal, ψ, by a linear combination of the wave functions $\{\phi_I\}$ of the elemental electronic states of molecules, like

$$\psi^{CI} = \sum_I C_I \phi_I. \tag{1}$$

Here, ϕ_I denotes a product of the various electronic states of the elemental molecules: for example, $\phi_I = \| \cdots \varphi_B^{(0)} \varphi_A^{(i)} \varphi_C^{(0)} \cdots \|$, where $\varphi_A^{(i)}$ is the ith electronic state of molecule A, $\varphi_B^{(0)}$ is the ground state of molecule B, etc. An important point is that we have to include all the electronic states of the component molecules, not only the ground states, but also their excited states, cation and anion states, and mixed states thereof. For example, a pair of cation and anion states describes an electron-transfer state and the intramolecular excited states describe so-called polarization states. If we include only the ground-state wave functions in Eq. (1), we would not be able to describe even the attractive interactions because of the exchange repulsions. These types of wave functions have been frequently used in the theory of chemical reactions and molecular interactions such as the frontier orbital theory of Fukui[34] and of Woodward and Hoffmann.[35] From the analysis of the component states ϕ_I that have large coefficients C_I, we can understand the nature of the interaction and the mechanism of the chemical reaction. For example, an electron-transfer interaction between the highest occupied molecular orbital (HOMO) of the reactant to the lowest unoccupied molecular orbital (LUMO) of another reactant often produces a driving force of the reaction.[34] However, in this formulation, if we want to be quantitative, a large drawback is size extensivity: a limited configuration interaction (CI)-type expansion does not satisfy the size extensivity. For this reason, we cannot adopt the CI-type expansion like Eq. (1) for the description of giant molecular systems.

To make the theory size extensive, we adopt the cluster-expansion formalism

$$\psi^{SAC} = \exp\left(\sum_I C_I S_I\right) \psi_0 \tag{2}$$

for describing the ground state of molecular crystal. Here, we limit our ground state to the closed-shell singlet. In connection with the CI-type expression given by Eq. (1), the component function ϕ_I is written as $\phi_I = S_I \psi_0$ where S_I is an operator that generates the component function ϕ_I when applied to ψ_0, the reference wave function. As in the original SAC expansion,[10,11] we take the operator S_I to be symmetry adapted, so that the number of the variables is to within those necessary for describing the pure singlet spin-space state.[11] The operator S_I describes intramolecular excitation that is polarization, intermolecular excitation that is electron transfer, and a coupling of them such as polarization electron transfer. We take ψ_0 to be an approximation to the Hartree-Fock wave function of the ground state of the molecular crystal. If we take ψ_0 as the antisymmetrized product of the Hartree-Fock determinants of the isolated molecules placed at the positions of the molecular crystal, we will have a strong repulsion due to the exchange repulsion. So, the directly interacting part between the nearest neighbor monomers of the system must be included from the beginning in the reference wave function ψ_0. The long-range Coulomb effects, etc, must also be included at this level, as will be described in more detail in the next section. Then, the correlation effects dealt with by the SAC method are essentially short range in nature, which makes the calculations of the correlation part easier than otherwise. The coefficients C_I are calculated by solving the following nonvariational equation:

$$\langle \psi_0 | (H - E) | \psi^{SAC} \rangle = 0 \tag{3}$$

and

$$\langle \psi_0 | S_J (H - E) | \psi^{SAC} \rangle = 0. \tag{4}$$

The present theory is a natural extension of the standard SAC theory originally proposed in 1978.[10] Equations (2)–(4) are just the same as those for the standard SAC theory for small and medium-size molecules.

Based on the SAC wave function, we next define the SAC-CI wave function of the giant molecular system by

$$\psi^{SAC-CI} = \sum_I d_K R_K \psi^{SAC}, \tag{5}$$

where R_K represents a singlet symmetry-adapted excitation operator, such as S_I in the SAC wave function, as well as the triplet excitation, ionization, and electron attachment operators. The coefficient d_K is calculated by solving the nonvariational equation,

$$\langle \psi_0 | R_K (H - E) | \psi^{SAC} \rangle = 0. \tag{6}$$

Again, the theoretical framework of the giant SAC-CI method is just the same as that of the standard SAC-CI method for smaller-size molecules.[11] So, we can make up our methodology to be continuous seamlessly from the standard method for small molecules to the method for giant molecular systems.

Similar to the CI case given by Eq. (1), the large coefficients C_I and d_K in the SAC and SAC-CI wave functions

FIG. 1. One-dimensional ring crystal composed of single molecular species A.

show the natures of the interactions and excitations and suggest the origins and the mechanisms of the chemical phenomena under considerations.

It is now clear that the building up of the theory consists of two parts: the definitions of the reference orbitals and wave function ψ_0 and the construction of the SAC/SAC-CI wave functions by defining the excitation operators S_I and R_K in Eqs. (2) and (5) with the use of the reference orbitals. Actually, the detailed setup of these two parts would be dependent on the systems under consideration. For example, molecular crystal, polymer, and biological protein would require different treatments, though a unified single treatment would become possible after the developments. In this first paper, we deal with the simplest possible such system, a cyclic molecular crystal composed of a single molecular species A.

III. REFERENCE WAVE FUNCTION FOR CYCLIC MOLECULAR CRYSTAL

We show in Fig. 1(a) an illustration of our cyclic molecular crystal. In this system, the strongest interactions would be within a molecule A_i and the next would be in the nearest neighbor intermolecular interactions between A_i and A_{i+1}. The non-neighboring interactions between A_i and A_{i+2} and A_i and A_{i+3} should be further and further smaller, since they are indirect and the distance becomes larger and larger.

Figure 1(b) is an illustration of our basic concept. Two neighboring monomers A-B represent the main interactions between the monomers. Here, B is actually the same species as A. The surrounding C regions mimic the real potential surrounding the representative dimer A-B. They also work to shield the potential due to the outside region D, which represents all the other part of the crystal and may be described by the electrostatic potential due to the gross charge distributions on the constituent atoms. For better approximations, we may include two, three, etc., monomers in the A and B regions. The formulation is almost the same as the present one.

A. Reference orbitals, wave function, and energy

First is the setup of the reference wave function ψ_0 and the component molecular orbitals used in the definition of the excitation operators in the SAC/SAC-CI wave functions. One choice would be the Hartree-Fock wave function of the cyclic molecular crystal itself. For giant molecular systems, some Hartree-Fock treatments were published: the elongation method by Fujimoto et al.[19] and Imamura et al.;[20] the fragment molecular orbital method by Kitaura and co-workers,[23] etc. We may use such methods at this stage, but the fragment MO method seems not to be useful for the present purpose because it is a method for calculating the energy, but not for the wave function. For the present purpose, however, we can introduce an easier method for constructing the reference orbitals and wave function of the giant SAC/SAC-CI method.

Now, we refer to the ring crystal shown in Fig. 1(b). This ring crystal is composed of the same monomer species A, so that the elemental parts A, B, C, and D of Fig. 1(b) are actually composed of the same monomer species A. We focus on the two neighboring monomers of the crystal and call them A and B. C includes several (M_C) monomers that are neighbors of either A or B. The monomers in C describe the real neighbors of A and B in the crystal and also work to shield the effect originating from D onto the central monomers A and B. D represents all the crystal molecules other than A, B, and C.

We perform Hartree-Fock calculations for the oligomers (M-mer) $CABC$, composed of $M = 2 + 2M_C$ monomers in the effect of D which is approximated as an electrostatic effect by putting the point gross charges on the constituent atoms obtained by the monomer calculation. The Hartree-Fock wave function for the present oligomer $CABC$ may be represented as

$$\phi_0 = \|_{DDD}\varphi_C\varphi_C\varphi_C\varphi_C\varphi_A\varphi_B\varphi_C\varphi_C\varphi_C\varphi_{CDDD}\|, \qquad (7)$$

where the wave function φ_A, etc., are the single determinant composed of the orbital i_A of A as

$$\varphi_A = \|\cdots i_A \alpha i_A \beta \cdots\| \qquad (8)$$

and D simply represents their electrostatic field. The real molecular orbitals in Eq. (7) are only those included in φ_A, φ_B, and φ_C. The orbitals i_A of φ_A of Eq. (8) are not the Hartree-Fock canonical orbitals of the oligomer $CABC$, but actually the ml-CMO defined below. Likewise, we have i_B of φ_B, etc. The ml-CMO's of A are, though the detailed definitions are given below, the orbitals that are unitary transformed from the canonical orbitals of $CABC$ and are similar to the canonical orbitals of the monomer A as designed to be so. The Hartree-Fock wave function ϕ_0 itself is invariant under these unitary transformations. The ml-CMO's of φ_A, φ_B, and φ_C satisfy orthonormality to each other. The orbitals i_A of φ_A, for example, extend not only within A but also to B and slightly to C. By symmetry, φ_A and φ_B are the same thing except for the coordinate centers of the orbitals.

With the use of φ_A and φ_B calculated above, we define the reference wave function ψ_0 for the SAC/SAC-CI calculations by

$$\psi_0 = \| \cdots \varphi_B \varphi_A \varphi_B \varphi_A \varphi_B \varphi_A \varphi_B \varphi_A \cdots \|. \qquad (9)$$

In the reference wave function, the orbitals of the nearest neighbor monomers A and B satisfy orthogonality condition to each other, but the orbitals of the monomers not adjacent to each other have overlaps, though they are small since the distance is already large and since the orbitals of φ_A and φ_C were originally orthogonal to each other in Eq. (7), and φ_C in Eq. (7), was an approximation of φ_A in that position of the ring crystal. We ignore these small overlaps. The energy E_0 of this reference function ψ_0 of the ring crystal composed of N monomers is written as

$$E_0 = E_A \times N, \qquad (10)$$

where E_A is given by

$$E_A = \sum_i^A 2H_{ii} + \sum_{i,j}^A (2J_{ij} - K_{ij}) + \sum_i^A \sum_j^B (2J_{ij} - K_{ij})$$
$$+ \sum_i^A \sum_j^{A',B'(C)} (2J_{ij} - K_{ij}). \qquad (11)$$

In the above equation, H_{ii} is the core-Hamiltonian matrix of the orbital i of A in the field of the bare nuclei of A, B, and C of Fig. 1(b) plus in the electrostatic field due to the gross charge distributions of the monomers in the D region of Fig. 1(b). A and B are the two neighboring monomers, and A' and B' denote the monomers A and B in the position of the right-hand-side C of Fig. 1(b). We include only the interactions from the right-hand side, and the interactions from the left-hand side are replaced with that of the right-hand side, from symmetry, since this is a better approximation. The integrals J_{ij} and K_{ij} are the ordinary Coulomb and exchange repulsion integrals between the orbitals i_A on A and the orbital j centered on either of the monomers of A, B, or C, depending on the second, third, and last terms of Eq. (11).

Thus, the reference wave function ψ_0 defined above for the present SAC/SAC-CI calculations is not the Hartree-Fock wave function of the ring crystal. However, it is actually a good approximation of the Hartree-Fock wave function. The approximation becomes better as the size of the C region increases, as will be examined later in Sec. V B. It is important that all the long-range interaction terms, such as Coulombic ones, must be included at the stage of the reference wave function. If the reference wave function is Hartree-Fock, this is done well: the correlation effects left are short range in nature, as shown clearly by Sinanoglu.[36] However, we note that in the SAC/SAC-CI formalism the reference wave function ψ_0 need not be the Hartree-Fock wave function. Thouless[37] proved that the coupled cluster theory including single excitation operators satisfy self-consistency, so that the Hartree-Fock accuracy is automatically obtained when the linked and unlinked terms of the single excitation operators are included in the formalism. The same is true for the SAC formalism. In the present calculations, we have included terms up to the product of the single operators, i.e., $|S(1)S(1)\rangle$, in the unlinked terms. Nevertheless, it is convenient if the reference orbitals are close to the Hartree-Fock orbitals.

In the above formalism, we assumed that all the monomers in the crystal are equivalent. However, we note that the above treatment is applicable with minor modifications even when A and B are different species. Further, even if the crystal is composed of the same molecular species, the neighboring monomers may be in different environments. For example, in the calculation of the water ring crystal given below, the H_2O molecules were arranged in an alternating way where two neighboring H_2O are in different environments. Such cases are easily included in the above formalism. For example, E_A of Eq. (10) is replaced with $(E_A + E_B)/2$, where E_B is calculated from Eq. (11) by exchanging the suffixes A and B. Further, the size of A or B can be enlarged if higher accuracy is necessary. For example, we may use a dimer for A or B instead of a monomer: A is actually AA in this case. Then, longer-range excitation operators are included in the SAC/SAC-CI stage, giving better accuracy.

B. Monomer-localized canonical molecular orbital (ml-CMO)

Since electron correlations are short-range phenomena, as clearly shown by Sinanoglu,[36] localized orbitals are more favorable than the delocalized orbitals for calculating electron correlation phenomena. If our purpose is the SAC calculation of the ground state alone, well-localized orbitals are thus favorable since electron correlations are efficiently described. In the SAC-CI calculations, however, we have to describe efficiently not only electron correlations, but also electron excitations. In molecular crystals, the interactions between monomers are weak, so that monomer pictures would be maintained even in the crystal. For describing electron excitations and ionizations, the canonical molecular orbital picture is a starting approximation, so that for the SAC-CI of molecular crystal, the adequate orbital would be the one that is localized essentially on each monomer and is similar to the canonical orbital of a free monomer. More delocalized or more localized orbitals are not adequate for the SAC/SAC-CI descriptions of both the ground, excited, and ionized states of molecular crystals.

Thus, for the SAC/SAC-CI calculations, the basic orbitals are preferable if they are similar to the canonical molecular orbitals (CMO's) of the monomer. This is also useful for retaining monomer pictures even in the crystal. However, the canonical Hartree-Fock orbitals of the M-mer, $CABC$ are much delocalized and are very different from the canonical orbitals of the monomer. When we apply the conventional localization method such as those of Boys[38] and Pipek-Mezey[39] to the CMO's of the M-mer, the resultant MO's are localized too much: they are very different from the CMO's of monomer, but similar to the localized molecular orbitals (LMO's) of the monomer. So, we have adopted the following localization procedure to obtain the orbitals similar to the CMO's of the monomer from the CMO's of the M-mer.

First, we transform the CMO's of the monomer into the LMO's by the Pipek-Mezey localization method and record the CMO-LMO transformation matrix U which is used in the

later step. Second, the CMO's of the M-mer are localized by the Pipek-Mezey method. Generally speaking, the LMO's of the M-mer have the shapes similar to the LMO's of the monomer, so that one can group the LMO's of the M-mer into each monomer component. Then, in the final third step, we backtransform each set of the grouped LMO's of the M-mer, using the transpose of the transformation matrix U^* calculated in the first step for the monomer localization procedure, into the set of the "canonical-like" orbitals of each monomer of the M-mer. This is done for both occupied and unoccupied MO's. We have confirmed that by this localization method, we could get the localized orbitals of the M-mer that have the shapes similar to those of the CMO's of the monomer. So, we call these localized orbitals as "monomer-localized canonical MO's" which we abbreviate as ml-CMO's. Since all the transformations done in the above processes are unitary transformations within the occupied or unoccupied manifolds, the total Hartree-Fock wave function of the M-mer is invariant under the transformations made in the above processes of calculating the ml-CMO's. Examples of the ml-CMO's are given later in Sec. V in comparison with the other CMO's and LMO's.

C. Integral transformation

After calculating the reference orbitals of the SAC/SAC-CI, the next step is the integral transformation of the basic integrals. We transform the atomic integrals into the molecular integrals using the ml-CMO's. When we designate these molecular integrals as $(i_A j_B | k_C l_D)$, where the suffixes A, B, C, and D denote the monomers to which the orbitals i, j, k, and l belong, we include only those integrals whose footing suffixes are within one monomer or within nearest neighbors. We neglect the integrals whose footing suffixes spread out of the nearest neighbor monomers. For example, we include $(i_A j_B | k_A l_B)$, but neglect $(i_A j_B | k_D l_A)$. This is due to the short-range nature of the electron correlations[36] to be considered in the next SAC/SAC-CI step. For the symmetry of the ring crystal considered here, the integral transformation is done only for the ml-CMO's of the central dimer of the $CABC$. Thus, only a single Hartree-Fock calculation of the M-mer $CABC$, the ml-CMO localization of the resultant MO's, and the integral transformation using the ml-CMO's of the central dimer alone are enough for calculating all the necessary integrals appearing in the Hamiltonian matrices for giant molecular crystal, independent of the size of the crystal. This is a big saving in contrast to the calculations of the whole system. If the integral including the C region like $(i_A j_A | k_C l_C)$ is large, it is better to include the C region into A or B regions from the beginning.

IV. SAC/SAC-CI WAVE FUNCTIONS FOR CYCLIC MOLECULAR CRYSTAL

Now, the reference wave function ψ_0 in the SAC wave function given by Eq. (2) has been defined. So, the next step is the definition of the excitation operators S_I and R_K
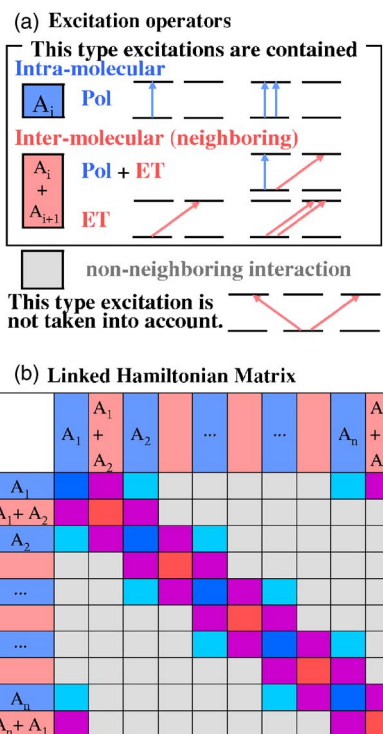
FIG. 2. (a) Single and double excitation operators contained in the giant SAC/SAC-CI method and (b) concepts of the linked Hamiltonian matrix of the present giant SAC/SAC-CI method.

included in the SAC wave function of Eq. (2) and the SAC-CI wave function of Eq. (5). These excitation operators are defined with the use of the ml-CMO's $\{i_A\}$, both occupied and unoccupied. Since the ml-CMO's have a local picture assigned to each monomer of the crystal, we can assign each excitation like from monomer A to monomer B in the crystal. When the excitation is within a monomer, we call it polarization type and when it is from one monomer to a neighboring monomer, it is referred to as electron transfer type.

In this first paper of the giant SAC/SAC-CI method, we include only singles and doubles excitation operators in the linked SAC operators S_I of Eq. (2) and the SAC-CI linked operators R_K of Eq. (5). We consider only the excitations within the neighboring monomer pairs, A_i and A_{i+1}. As one-electron operators, we consider one-electron excitations within monomer (polarization: pol) and one-electron transfers (ET) to the neighboring monomer. As two-electron operators, we consider two-electron excitations within monomer (double pol), polarization plus electron transfer (pol+ET), and two-electron transfers (double ET) between A_i and A_{i+1}, as illustrated in Fig. 2(a). Simultaneous one-electron transfers to the two different neighboring monomers were not taken into account in the present study. The excitations involving non-neighboring pairs were disregarded. As in the ordinary SAC/SAC-CI calculations, the perturbation selection was done for the linked operators in order to keep only the important operators in the SAC/SAC-CI calculations.[12]

The SAC/SAC-CI Hamiltonian matrix elements derived from Eqs. (4) and (6) may be written as[11,12]

$$G_{IJ} = \langle I|H|J\rangle + \tfrac{1}{2}\sum_K C_K \langle I|H|JK\rangle$$

$$+ \tfrac{1}{6}\sum_{K,L} C_K C_L \langle I|H|JKL\rangle$$

$$+ \tfrac{1}{24}\sum_{K,L,M} C_K C_L C_M \langle I|H|JKLM\rangle. \qquad (12)$$

The first term is the linked term and the other terms are the unlinked terms. The suffixes I and J denote either the SAC operators S_I and S_J or the SAC-CI operators R_I and R_J. The suffices K, L, and M denote the SAC operators S_K, S_L, and S_M. As described above, these operators generate polarization configurations, electron-transfer configurations, etc., on applying the zeroth order wave function ψ_0 of the crystal. The suffixes I and J also refer to these configurations. The linked and unlinked integrals are reduced to the sums of the one-electron integrals h_{ij} and the two-electron integrals $\langle ij|kl\rangle$ composed of the ml-CMO's, i and j. Here, we keep only such integrals whose component orbitals all fall into the two neighboring monomers of the crystal. The SAC energy is calculated from Eq. (3) as

$$E_{\mathrm{SAC}} = E_0 + \sum_I C_I \langle 0|H|I\rangle + \sum_{I,J} C_I C_J \langle 0|H|IJ\rangle, \qquad (13)$$

where I in the first term represents both single and double excitations and I and J in the second term represent both single excitations. Note again that our reference wave function ψ_0 is not strictly the Hartree-Fock wave function.

The Hamiltonian matrix of the linked operators, $H_{IJ} = \langle I|H|J\rangle$, of the present system may be illustrated as shown in Fig. 2(b). It is composed of only four distinct blocks for the symmetry of the present system because we consider two types of linked operators; polarization operators within A_i and electron-transfer operators A_i and A_{i+1}. The diagonal blocks are classified by the nature of the linked operators, I.

(1) The diagonal blue block represents the matrix elements between the polarization operators within A_i.
(2) The diagonal red block represents the matrix elements between the electron-transfer operators between A_i and A_{i+1}.

The off-diagonal blocks are classified by the natures of the linked operators I and J.

(1) The purple block represents the Hamiltonian matrix between the polarization operators and the electron transfer operators between A_i and A_{i+1}.
(2) The light-blue block represents the off-diagonal matrix elements between the polarization operators in the different neighboring sites.

The gray regions represent the non-neighboring interactions that should be much smaller than the other colored blocks, since electron correlations are short-range: they were approximated to be zero here. In other words, the linked integrals in the gray blocks reduce to the molecular integrals whose MO-footing monomer indices extend out of the nearest neighbor A-B region, so that they are neglected to be small. Thus, because of the symmetry of the system, we have

to calculate only the colored four blocks, independent of the size of the ring crystal. This is certainly a big saving.

Next is the calculation of the unlinked terms, the second to the last terms of Eq. (12). These unlinked terms are very important to guarantee the size extensivity of the energy. We therefore included almost all the important unlinked terms composed of the linked terms selected at the beginning of the calculations. Among all possible unlinked terms constructed from all the singles and doubles excitation operators, the terms including higher-order contributions of the single excitation SAC operators, $S(1)$, are usually very small. Therefore, we included in the SAC calculations only the unlinked terms $|S(2)S(2)\rangle$, $|S(2)S(1)\rangle$, and $|S(1)S(1)\rangle$, dropping out the unlinked terms $|S(1)S(1)S(1)\rangle$, $|S(2)S(1)S(1)\rangle$, and $|S(1)S(1)S(1)S(1)\rangle$, where $S(2)$ denotes double excitation SAC operator. In the SAC-CI calculations, we included only $|R(1)S(2)\rangle$, $|R(2)S(2)\rangle$, $|R(1)S(1)\rangle$, and $|R(2)S(1)\rangle$, neglecting the terms $|R(1)S(1)S(1)\rangle$, $|R(2)S(1)S(1)\rangle$, $|R(1)S(2)S(1)\rangle$, and $|R(1)S(1)S(1)S(1)\rangle$, where S is the SAC operator and R is the SAC-CI operator. Among the neglected terms, the term $|R(1)S(2)S(1)\rangle$ for the SAC-CI calculations may be larger than the other neglected terms and therefore would be included in the future calculations. Thus, in the present approximation, the SAC/SAC-CI Hamiltonian matrix elements given by Eq. (12) are simplified as

$$G_{IJ} = \langle I|H|J\rangle + \tfrac{1}{2}\sum_K C_K \langle I|H|JK\rangle. \qquad (14)$$

The unlinked integrals appear in the Hamiltonian matrix shown in Fig. 2 not only in the colored blocks, but also in the gray blocks. For example, in the diagonal block of the SAC/SAC-CI calculations, we have the integrals

$$G_{I_A I_A} = H_{I_A I_A} + \tfrac{1}{2}\sum_{K_D} C_{K_D} \langle I_A|H|I_A K_D\rangle = H_{I_A I_A}$$

$$+ \tfrac{1}{2}\sum_{K_D} C_{K_D} \langle 0|H|K_D\rangle, \qquad (15)$$

where $|0\rangle$ represents the reference wave function ψ_0. So, in the blue matrix elements within the monomer A, $G_{I_A I_A}$, the unlinked contributions from the distant monomer D arise. Furthermore, in the off-diagonal matrix element $G_{I_A K_D}$ between the operators of A and D, which lies in the gray region of the matrix shown in Fig. 2, the following unlinked term appears

$$G_{I_A K_D} \supset \tfrac{1}{2} C_{I_A} \langle I_A|H|I_A K_D\rangle = \tfrac{1}{2} C_{I_A} \langle 0|H|K_D\rangle. \qquad (16)$$

Namely, even in the off-diagonal block between the distant monomers A and D, $G_{I_A K_D}$, we have the contributions of the unlinked integrals. By including all such unlinked terms, the size extensivity and the size intensivity of the calculated results are guaranteed.

In this way, with the ml-CMO's of a single central dimer of the M-mer, A-B of Fig. 1(b), all the matrix elements of the giant molecular ring crystal are calculated. As far as the integral evaluation is concerned, a single M-mer calculation is enough in the present approximation, independent of how large the molecular ring crystal is. The self-consistent field calculation of only the M-mer, the integral transformation with the ml-CMO's of the central dimer alone, and the per-

turbation selection of the linked operators involving only these central dimer ml-CMO's are all quite rapid in comparison with the calculations of the whole ring crystal. In the standard SAC/SAC-CI method, however, even the Hartree-Fock calculations and the integral transformations soon become impossible as the size of the crystal increases.

In this paper, we describe our methodologies and give an actual example of one-dimensional ring crystals. Our methodology is general and easily extended to three-dimensional molecular crystals. Because of the short-range nature of electron correlations, the sparse structures of the matrices, as illustrated in Fig. 2(b), is retained even for three-dimensional systems.

The standard SAC/SAC-CI code was rewritten recently for accelerating the integral evaluations of both the linked and unlinked parts. We have introduced a new direct algorithm[40] that does not require the use of the projective reduction[41] routines and at the same time permits the perturbation selection of the linked excitation operators at the beginning of the calculations. This new algorithm has served not only to accelerate the calculations, but also to eliminate the approximations existing in the evaluations of the unlinked integrals of the old version. The latter improvement was important in the present giant code particularly for obtaining the correct size extensivity.

For the diagonalization of the nonsymmetric SAC and SAC-CI equations, we used the conventional iterative procedure[42] that are incorporated in the SAC-CI part of GAUSSIAN 03. It is possible to improve this diagonalization part considering the nature of the systems under consideration. We plan to accelerate this diagonalization part in the future for large scale applications of the present method to really interesting systems.

V. APPLICATIONS: SETUP OF REFERENCE ORBITALS AND WAVE FUNCTION

Now, we apply the method summarized above to actual systems. We examine the basic ideas adopted in the present calculations. In the Hartree-Fock calculations of *CABC* shown in Fig. 1(b), only one monomer was assigned to *C*, so that our *CABC* is a tetramer, which is the lowest-order approximation. First, we did the Hartree-Fock calculation of the monomer and obtained the atomic gross charges that are used for the electrostatic approximation of region *D*. Then, we performed the Hartree-Fock calculation for the tetramer *CABC*. Outside the tetramer, which is region *D*, we put the gross charge distributions of the crystal molecules of the ring crystal, which affects the electronic structure of the tetramer through the electrostatic interactions. The Hartree-Fock canonical orbitals of the tetramer were then transformed into the ml-CMO's for preparing the reference wave function of the SAC/SAC-CI calculations. There, we used the Pipek-Mezey (PM) localization method.[39] The present ml-CMO's thus extend over the tetramer of the crystal. In all calculations, we optimized the monomer geometry with the basis set used, and the ring crystal was constructed using these monomers.
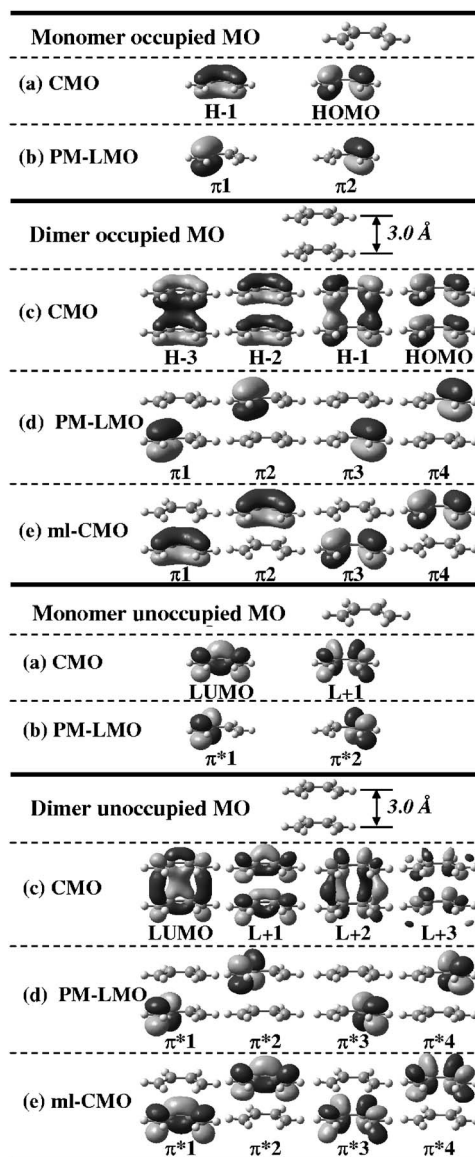

FIG. 3. π orbitals of butadiene monomer: (a) CMO and (b) PM-LMO, and of butadiene dimer: (c) CMO, (d) PM-LMO, and (e) ml-CMO.

A. ml-CMO's of butadiene dimer

Before entering into details, we compare the CMO's, LMO's, and ml-CMO's of the weakly interacting butadiene dimer separated by 3 Å calculated with the D95 basis for understanding the nature of the ml-CMO's. In Fig. 3, we show the occupied and unoccupied π orbitals of butadiene monomer: (a) the canonical orbitals (CMO's) and (b) the PM LMO's. For the dimer, (c) shows the CMO's that are delocalized over the dimer and different from the CMO's of the monomer. The PM-LMO's of the dimer are shown in (d) and are localized just like the PM LMO's of the monomer but are different from the CMO's of the monomer. Similarly, other PM σ-LMO's of the dimer were quite different from the CMO's of the monomer. On the other hand, the ml-CMO's shown in (e), which were calculated by the method reported in Sec. III B, are very similar to the CMO's of the monomer, as expected. We have confirmed that this was true not only for the π orbitals but also for the other σ orbitals.

TABLE I. Energy of the reference wave function (ψ_0) compared with the Hartree-Fock wave function.

M_C[a]	H$_2$O			C$_2$H$_4$		
	ψ_0 (a.u.)	Hartree-Fock (a.u.)	Δ[b] (a.u.)	ψ_0 (a.u.)	Hartree-Fock (a.u.)	Δ[b] (a.u.)
1	−760.129 404	−760.130 760	0.001 356	−780.110 026	−780.110 214	0.000 188
2	−760.130 962	−760.130 760	−0.000 202	−780.110 191	−780.110 214	0.000 023
3	−760.130 653	−760.130 760	0.000 107	−780.110 207	−780.110 214	0.000 007
4	−760.130 760	−760.130 760	0.000 000	−780.110 214	−780.110 214	0.000 000

[a]Number of monomers included in the C region.
[b]The error between ψ_0 and Hartree-Fock.

B. Comparison of the present reference wave function with the Hartree-Fock wave function

Now, we examine how close our reference wave function ψ_0 is to the Hartree-Fock wave function of the molecular crystal. Though this is not necessary for the construction of the present theory, because the SAC formalism includes automatically the self-consistency (Thouless theorem[37]) though partially here for some approximations introduced, it is convenient if our ψ_0 is close to the Hartree-Fock wave function. We calculated the Hartree-Fock wave function of a small ring crystal composed of water 10-mer with the interwater distance of 3.0 Å using the D95 basis set. We compared it with the present ψ_0 obtained with the use of different sizes for the C region. Similar calculations were also done for ethylene 10-mer with the interwater distance of 4.5 Å using the D95 basis set. Table I summarizes the results, where M_C is the number of the monomers included in the C region. When $M_C=1$, $CABC$ is tetramer and when $M_C=4$, $CABC$ is 10-mer, the whole ring crystal. When $M_C=1$, the energy difference Δ between the present ψ_0 and the Hartree-Fock is 1.36 mhartree for water and 0.19 mhartree for ethylene, and when $M_C=2$, Δ decreases considerably and as M_C increases, Δ becomes very small. Note that at $M=4$, Δ should be zero. Δ is consistently smaller for ethylene than for water, since ethylene is essentially nonpolar but water is polar. Further, the present approximation for the $CABC$ part would become better as the size of the ring crystal increases, since the indirect monomer interactions decrease as the size of the ring crystal increases.

When the reference function is Hartree-Fock, the one-electron excitation operator does not contribute to the SAC energy given by Eq. (13). We checked such contributions of the single excitation operators for the $M_C=1$ case of 10-mer for both water and ethylene. The contribution to the second term was essentially zero for both water and ethylene and the contributions to the last term were 0.000 930 and 0.000 010 hartree for water and ethylene, respectively, which are also very small. Thus, the present reference wave function is close to the Hartree-Fock wave function.

VI. SIZE EXTENSIVITY, SIZE INTENSITY, AND ACCURACY

A. Size extensivity check for H$_2$ crystal

Size extensivity is a very important requirement for the theory dealing with large molecular systems since otherwise, we cannot study energetic properties of the system. Here, we check the size-extensivity of the present SAC method using the simplest example of H$_2$ crystal. We calculate cyclic crystal composed of 10–10 000 monomers. The distance between the adjacent monomers is 100.0 Å, which implies that essentially no interactions exist between the monomers. The basis set is D95 and no perturbation selection was performed. Since the atomic gross charge of the monomer is zero, the electrostatic contribution vanishes identically.

Table II shows the total energies of the H$_2$ ring crystals of various sizes calculated by the SDCI and SD-SAC methods. The term Δ_{SDCI} and Δ_{SAC} give the size-extensivity error of the SDCI and SAC methods; $\Delta=E(N\text{-mer})-N \times E(\text{monomer})$. For a single H$_2$ molecule that includes only

TABLE II. Size-extensivity check of the SDCI and SAC methods for the noninteracting H$_2$ ring crystal of size N.

N[a]	Giant[b]		Monomer$\times N$ (a.u)	Δ_{SDCI}[c] (a.u)	Δ_{SAC}[d] (a.u)
	SDCI (a.u)	SAC (a.u)			
1	−1.151 349	−1.151 349	−1.151 349		
10	−11.488 501	−11.513 492	−11.513 492	0.024 990	0.000 000
20	−22.939 618	−23.026 983	−23.026 983	0.087 365	0.000 000
100	−114.079 011	−115.134 916	−115.134 916	1.055 905	0.000 000
1000	−1132.724 779	−1151.349 157	−1151.349 158	18.624 378	0.000 000
10000	−11287.943 813	−11513.491 575	−11513.491 576	225.547 764	0.000 001

[a]Number of monomers in the ring crystal.
[b]Giant SAC/SAC-CI program.
[c]Size-extensivity error of the giant SDCI calculation.
[d]Size-extensivity error of the giant SAC calculation.

TABLE III. Size-extensivity check and timing for the noninteracting H_2 crystal using giant and standard SAC programs.

N[a]	Standard[b]		Giant[c]		Monomer$\times N$ (a.u.)	$\Delta_{standard}$[d] (a.u.)	Δ_{giant}[e] (a.u.)
	Total energy (a.u.)	Wall clock (s)	Total energy (a.u.)	Wall clock (s)			
1	−1.151 349		−1.151 349		−1.151 349 157 6		
10	−11.513 492	271	−11.513 492	29	−11.513 492	0.000 000	0.000 000
20	−23.026 983	3495	−23.026 983	30	−23.026 983	0.000 000	0.000 000
100			−115.134 916	31	−115.134 916		0.000 000
1000			−1 151.349 157	67	−1 151.349 158		0.000 000
10000			−11 513.491 575	546	−11 513.491 576		0.000 001

[a]Number of monomer.
[b]Standard SAC/SAC-CI program.
[c]Giant SAC/SAC-CI program.
[d]Size-extensivity error of the standard SAC calculation.
[e]Size-extensivity error of the giant SAC calculation.

two electrons, the SDCI is full CI and so is the SAC. As the number of the monomers, N, increases, the size-extensivity error of the SDCI method increases and amounts to as large as 225 a.u. (1.4×10^5 kcal/mol) for $N = 10\,000$. This number is extraordinarily large in a chemical sense: when we calculate strongly interacting H_2 crystals with the SDCI method, we have no way to distinguish the true interaction energy and the size-extensivity error, and therefore we cannot do any chemistry at all. On the other hand, with the SAC method, the size-extensivity error is quite small: even for the crystal of $N = 10\,000$, $\Delta_{SAC} = 0.001$ mhartree (0.0006 kcal/mol) within the total energy as large as −11 513.492 hartree. Therefore, even for the giant molecular crystals, we can do the discussions of kcal/mol accuracy with the SAC method, which is very important for doing chemistry. In summary, Table II shows how large the size-extensivity error is in the SDCI method and how important the size-extensivity requirement is for the theory of large molecular systems.

Table III shows a comparison of the present giant SAC method with the standard SAC method, both with the new direct algorithm,[40] and $\Delta_{standard}$ and Δ_{giant} give the size-extensivity errors of the corresponding methods. With the SAC method, the size-extensivity errors are very small for both methods, but the wall clock times of the giant and standard methods are very different. It takes only 546 s for the crystal of $N = 10\,000$ with the giant SAC method, but it takes 3495 s for the crystal of only $N = 20$ with the standard SAC

method. (This slowness of the standard SAC calculation is partly due to the fact that we did not do perturbation selection in this calculation.) The giant SAC method is much faster than the standard SAC method and the accuracy is similar. Therefore, the giant SAC method is potentially very useful.

B. Size-extensivity and size-intensivity check for C_2H_4 crystal

We will study ethylene ring crystal in Sec. VII A below, and here we check the size extensivity for the ethylene crystal before the chemical interaction is switched on, separating the interethylene distance to 100.0 Å. The basis set was D95 and the selection level in the SAC/SAC-CI calculations was level 2.[12] We included all the MO space as active except for the 1s core orbitals of carbons.

Table IV shows the size-extensivity check for the SDCI and SAC total energies. Again, the size-extensivity error Δ_{SAC} of the SAC method is as small as −0.13 mhartree (0.08 kcal/mol) even for the ethylene crystal composed of 1000 monomers. If we include all the unlinked terms, the error should be zero and even in the present approximation, Δ_{SAC} is completely negligible in a chemical accuracy. We can discuss chemical stability, such as geometry, chemical interaction, etc., of even the ethylene 1000-mer ring crystal. This is very important for chemistry researches of molecular

TABLE IV. Size extensivity check and timing of the SDCI and SAC methods for the noninteracting ethylene ring crystal of size N.

N[a]	SAC				SDCI	
	Total energy (a.u.)	Wall clock (s)	Monomer$\times N$ (a.u.)	Δ_{SAC}[b] (a.u.)	Total energy (a.u.)	Δ_{SDCI}[c] (a.u.)
1	−78.198 557		−78.198 557 301	0.000 000	−78.185 734	0.000 000
10	−781.985 573	203	−781.985 573	0.000 000	−781.307 923	0.549 416
20	−1 563.971 152	221	−1 563.971 146	−0.000 006	−1 562.182 638	1.532 040
50	−3 909.927 882	345	−3 909.927 865	−0.000 017	−3 904.129 264	5.157 431
100	−7 819.855 752	1 050	−7 819.855 730	−0.000 022	−7 806.571 808	12.001 582
1000	−78 198.557 434	17 950	−78 198.557 301	−0.000 134		

[a]Number of monomers in the ring crystal.
[b]Size-extensivity error of the giant SAC calculation.
[c]Size-extensivity error of the giant SDCI calculation.

TABLE V. Size-intensivity check of the excitation energy of the noninteracting C_2H_4 50-mer ring crystal.

Excited state	Excitation energy (eV)		Δ_{giant} [b] (eV)
	Giant[a]	Monomer	
1	9.0613	9.0593	0.0020
2	9.0613	9.0593	0.0020
3	9.0613	9.0593	0.0020
⋯	9.0613	9.0593	0.0020
⋯	9.0613	9.0593	0.0020
48	9.0613	9.0593	0.0020
49	9.0613	9.0593	0.0020
50	9.0613	9.0593	0.0020

[a]Giant SAC/SAC-CI program.
[b]Size-intensivity error of the giant SAC calculation.

crystal. However, on the other hand, the size-extensivity error Δ_{SDCI} of the SDCI method is extremely large: it amounts to as large as 12.002 a.u. (7531 kcal/mol) already for $N=100$. We can never do energetic chemical arguments of the giant system with the SDCI method.

We next study the excited states of the ethylene ring crystal with the giant SAC-CI method. The size intensivity of the excitation energy was examined for $N=50$ ring crystal, keeping $R=100.0$ Å, where essentially no interaction exists between the monomers. Table V shows the comparison of the lower 50 excitation energies of the ring crystal with the lowest excitation energy of the monomer. These are $\pi \rightarrow \pi^*$ excitations. The 50 excited states have degenerate excitation energies of 9.0613 eV, which is in good agreement with the excitation energy of the monomer (9.0593 eV). The small error 0.0020 eV (0.046 kcal/mol) arises. This error is probably due to the neglect of the unlinked term $|R(1)S(2)S(1)\rangle$ in the SAC-CI calculations. The calculated excitation energy

itself does not agree with the experimental value (about 8.0 eV),[43] since the basis set is not good enough for quantitative arguments (see Ref. 43 for detailed SAC-CI calculations of ethylene).

C. Comparison between giant and standard SAC/SAC-CI results

We must check now the accuracy of the giant SAC/SAC-CI method in the region near the equilibrium inter-monomer distance of the ring crystal. We calculated water and ethylene ring crystals of $N=10$ with the intermonomer distances of $R=3.0$ Å and $R=4.5$ Å, respectively. These systems are very small in comparison the above examples, but for the standard SAC-CI program, this size is already moderate. The basis set was D95 and the selection level in the SAC/SAC-CI calculations was level 2.[12] Ethylene was put parallel and water antiparallel to each other, as shown in Fig. 4. (We showed only the figure of 50-mer for ethylene.) Note that in this arrangement, two neighboring waters are in different environments. The ground-state total energy and the excitation energies are compared in Tables VI and VII for water and ethylene ring crystals, respectively.

The total energy of the water 10-mer ring crystal was calculated to be $-761.420\,922$ a.u. with the giant SAC method, which is different by only $0.001\,283$ a.u. (0.8082 kcal/mol) from the one ($-761.422\,206$ a.u.) with the standard SAC method. When the size of the C region (M_C) is increased from one to four monomers, the calculated total energy of the giant SAC method becomes closer to the total energy of the standard method for the 10-mer itself. The difference Δ shown in Table VI decreases from $0.001\,283$ to $-0.000\,051$ a.u.

Table VI also shows the lower ten excitation energies of the water crystal for different sizes of the C region. The

TABLE VI. Total energy, excitation energies, and wall clock timing for the H_2O 10-mer ring crystal.

| M_C [d]	Giant[a]				Standard[b]	Δ [c]			
	1	2	3	4		1	2	3	4
	Total energy (a.u.)								
$X\,^1A$	−761.420 922	−761.422 377	−761.422 047	−761.422 256	−761.422 206	0.001 283	−0.000 171	0.000 158	−0.000 051
	Excitation energy (eV)								
$1\,^1A$	8.530	8.527	8.527	8.527	8.545	−0.015	−0.018	−0.018	−0.018
$2\,^1A$	8.565	8.563	8.563	8.562	8.591	−0.026	−0.029	−0.028	−0.029
$3\,^1A$	8.565	8.563	8.563	8.562	8.592	−0.027	−0.030	−0.030	−0.030
$4\,^1A$	8.660	8.657	8.657	8.657	8.694	−0.034	−0.037	−0.037	−0.037
$5\,^1A$	8.660	8.657	8.657	8.657	8.693	−0.034	−0.037	−0.036	−0.037
$6\,^1A$	8.779	8.776	8.777	8.776	8.812	−0.033	−0.036	−0.036	−0.036
$7\,^1A$	8.779	8.776	8.777	8.776	8.813	−0.034	−0.036	−0.036	−0.036
$8\,^1A$	8.877	8.874	8.874	8.874	8.904	−0.027	−0.030	−0.030	−0.030
$9\,^1A$	8.877	8.874	8.874	8.874	8.905	−0.028	−0.031	−0.031	−0.031
$10\,^1A$	8.915	8.912	8.912	8.912	8.940	−0.025	−0.028	−0.028	−0.028
Wall clock	2 min, 24 s	2 min, 30 s	2 min, 45 s	3 min, 12 s	44 min, 48 s				

[a]Giant SAC/SAC-CI program.
[b]Standard SAC/SAC-CI program.
[c]The difference between the energies calculated by the giant and standard version programs.
[d]Number of monomers included in the C region.

TABLE VII. Total energy, excitation energies, and wall clock timing for the C_2H_4 10-mer ring crystal.

M_C[d]	Giant[a]				Standard[b]	Δ[c]			
	1	2	3	4		1	2	3	4
				Total energy (a.u.)					
$X\,^1A$	−781.980 077	−781.980 241	−781.980 259	−781.980 266	−781.980 173	0.000 096	−0.000 069	−0.000 087	−0.000 093
				Excitation energy (eV)					
$1\,^1A$	8.534	8.534	8.534	8.534	8.630	−0.096	−0.096	−0.096	−0.096
$2\,^1A$	8.616	8.616	8.616	8.616	8.681	−0.065	−0.065	−0.065	−0.065
$3\,^1A$	8.616	8.616	8.616	8.616	8.678	−0.062	−0.062	−0.062	−0.062
$4\,^1A$	8.827	8.827	8.827	8.827	8.815	0.011	0.012	0.012	0.012
$5\,^1A$	8.827	8.827	8.827	8.827	8.819	0.008	0.008	0.008	0.008
$6\,^1A$	9.081	9.081	9.081	9.081	9.014	0.067	0.067	0.067	0.067
$7\,^1A$	9.081	9.081	9.081	9.081	9.011	0.070	0.070	0.070	0.070
$8\,^1A$	9.283	9.283	9.283	9.283	9.211	0.072	0.072	0.072	0.073
$9\,^1A$	9.283	9.283	9.283	9.283	9.214	0.069	0.070	0.070	0.070
$10\,^1A$	9.360	9.360	9.360	9.360	9.332	0.027	0.027	0.027	0.027
Wall clock	15 min, 2 s	15 min, 2 s	19 min, 4 s	27 min, 51 s	1 d, 22 h, 55 min, 56 s				

[a]Giant SAC/SAC-CI program.
[b]Standard SAC/SAC-CI program.
[c]The difference between the energies calculated by the giant and standard version programs.
[d]Number of monomers included in the C region.

differences are within about 0.04 eV for all different ten excitations. The difference Δ of the excitation energy does not become smaller as the size of the C region increases, in contrast to the ground-state energy. This is due to the non-neighboring interactions that are different between the ground and excited states: they were neglected in the giant SAC-CI calculations but were included in the standard calculations.

For the ethylene 10-mer crystal, summarized in Table VII, the total energy difference between the giant and standard SAC methods was as small as 0.000 096 a.u. (0.0602 kcal/mol). When we enlarged the C region in the giant SAC calculations, this difference did not change much. The ten $\pi \rightarrow \pi^*$ excited states of 10-mer calculated by the giant SAC-CI method were different from those of the standard SAC-CI calculations to within 0.1 eV, and these differences were not improved by enlarging the size of the C region in the giant calculations. So, these differences are attributed to the long-range interactions that are more important in the excited states than in the ground state. However, we note that these long-range interactions arose partially due to the smallness of the system. In the small ring crystal, the non-neighboring interactions between the monomers are larger than in the large crystals, particularly in the excited states that are more diffuse in nature than the ground state. These interactions are included in the standard method but approximated by the point-charge interactions in the giant SAC/SAC-CI method.

Timing comparisons between the giant and standard methods given in Tables VI and VII are impressive. For the water crystal, the wall clock time for the giant SAC/SAC-CI calculation was 2–3 min, in comparison with 44 min, 48 s

for the standard calculations. For the ethylene crystal, this difference is much more impressive: the former was 15–27 min, in contrast to the latter, 1 d, 22 h, 56 min. Thus, the giant SAC/SAC-CI method is very fast and yet has a reasonable accuracy. It shows much potentiality of the present giant SAC/SAC-CI method for the theoretical studies of giant molecular crystals.
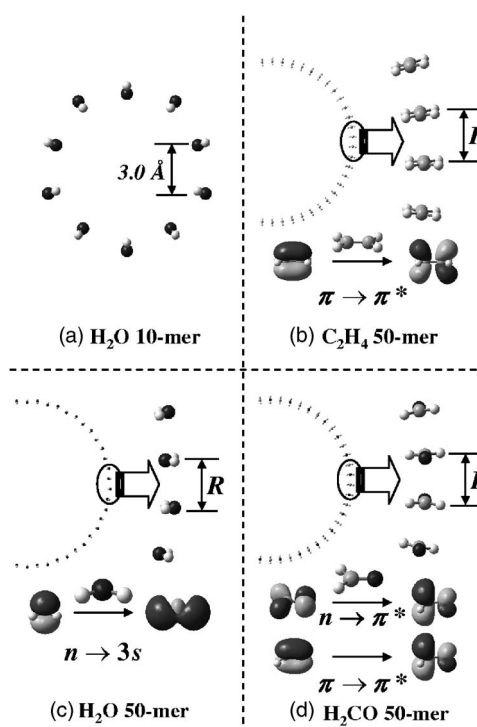
FIG. 4. The geometries and the target excited states of ring crystals: (a) H_2O 10-mer, (b) C_2H_4 50-mer, (c) H_2O 50-mer, and (d) H_2CO 50-mer.
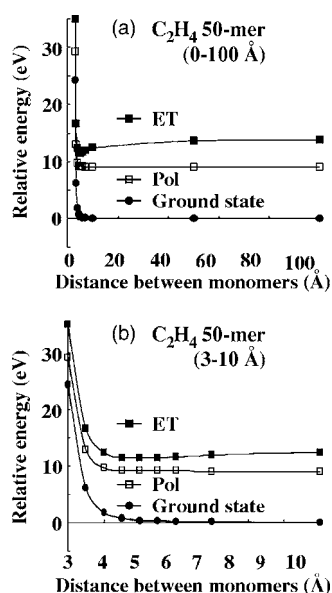
FIG. 5. The potential energy curves of the ground, polarization (Pol)-type, and electron-transfer (ET)-type $\pi \rightarrow \pi^*$ excited states of C_2H_4 50-mer: (a) 0–100 Å and (b) 3–10 Å.
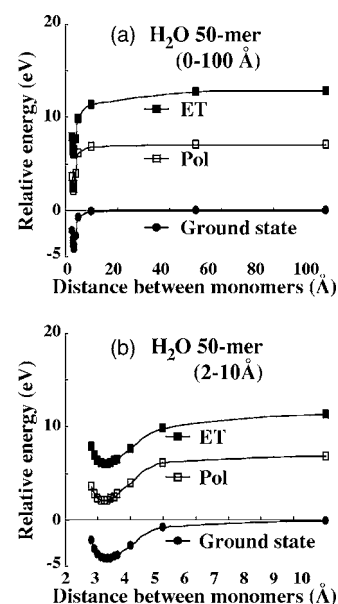

FIG. 6. The potential energy curves of the ground, polarization (Pol)-type, and electron-transfer (ET)-type $n \rightarrow 3s$ excited states of H_2O 50-mer: (a) 0–100 Å and (b) 2–10 Å.

VII. POTENTIAL ENERGY CURVES OF THE GROUND AND EXCITED STATES OF RING CRYSTALS

A. C_2H_4 ring crystal

Now, we apply the present giant SAC/SAC-CI method to some realistic chemical systems. As a simplest crystal having π orbital bands, we applied the present method to the ethylene ring crystal composed of 50 molecules, as shown in Fig. 4(b). Ethylenes interact side by side with each other and form a ring crystal. The basis set was D95 and the selection level in the SAC/SAC-CI calculations was level 2.[12] We included all the MO's as active space except for the 1s core orbitals. Because of the basic importance of ethylene in the spectroscopy of organic molecules, we have investigated this molecule several times by the SAC/SAC-CI method.[12,43]

The potential energy curves of the ground and excited states of the ethylene ring crystal were calculated by varying R, the interethylene distance defined in Fig. 4(b), from 3.0 to 100.0 Å and were shown in Fig. 5. At this level of approximation, the ground state was not attractive: the potential curve shows that the system is essentially noninteracting. The lower excited states of this crystal were polarization type, i.e., $\pi \rightarrow \pi^*$ excitations within each monomer. Since this excitation occurs essentially within each monomer, the excitation energy was rather independent of the interethylene distance. The repulsive nature was weaker in the 3.5–5 Å region than the ground state: this was partially due to the mixing of the polarization and electron-transfer types in the smaller region of R. Above these polarization-type states, there appeared the electron-transfer type $\pi \rightarrow \pi^*$ states: one electron transfer from the π orbital of an ethylene to the π^* orbital of the adjacent ethylene. This interethylene electron transferred state was attractive and had a minimum at around 4.90 Å. The depth of the potential minimum was 2.36 eV. Thus, the excitations of the ethylene ring crystal to the electron-transfer-type excited states would cause a shrink of

the crystal. The attractive force in the electron-transfer $\pi \rightarrow \pi^*$ state is due mainly to two origins: one is the Coulomb force between the positive and negative charges spread over each neighboring ethylene, and the other is the overlap forces between the two π and two π^* orbitals of the neighboring ethylenes.

B. H_2O ring crystal

We next study the H_2O ring crystal by the giant SAC/SAC-CI method. Free water molecule studied by this method[11,45] many years ago may be a good reference. We calculated the ring crystal composed of 50 molecules. They were arranged in an alternating way as shown in Fig. 4(c), so that the neighboring monomers are in different environments. This arrangement would be favorable from the dipole-dipole interaction between the monomers. The basis set was D95, and a set of Rydberg s,p functions[44] with the exponents of 0.032 (s) and 0.028 (p) were added to the two central oxygen atoms of the tetramers $CABC$. The selection level in the SAC/SAC-CI calculations was level 2.[12] We included all the MO's in an active space except for the 1 s core orbitals of oxygen. The Rydberg MO's of the tetramer localized by the Pipek-Mezey method were different from those of the monomer localized by the same method for the interwater distances less than 5.0 Å, since the Rydberg orbitals spread over two central monomers. So, we used the Pipek-Mezey LMO's for the Rydberg orbitals of the tetramer. The potential energy curves for the ground and excited states of the ring crystal against the variation of the interwater distance R are shown in Fig. 6, while Table VIII shows the potential properties and the vertical excitation energies.

First, we examine vertical excitation energy. At the intermonomer distance $R=100$ Å, the calculated vertical excitation energy (7.013 eV) for the excitation from the nonbonding π orbital of water to the 3 s Rydberg state was in

TABLE VIII. Potential properties and vertical excitation energies of the H_2O 50-mer ring crystal.

		R_e[a] (Å)	ω_e[b] (cm^{-1})	Depth[c] (eV)	Vertical excitation energy (eV)			
					$R=R_e$[d]	$R=100.0$[d]	Monomer	Expt.[e]
Ground state		3.26	477	4.231				
Excited states	Pol[f]	3.20	493	4.958	6.308	7.013	7.041	7.4
	ET[g]	3.23	488	6.845	10.217	12.827	12.947	

[a]Equilibrium distance between monomers.
[b]Vibrational frequency.
[c]The depth of potential energy curves.
[d]The distance between monomers.
[e]Reference 45.
[f]Polarization type.
[g]Electron transfer type.

good agreement with that of the monomer (7.041 eV). However, the agreement with the experimental value 7.4 eV (Ref. 46) is not good because the basis set used here is not good enough for studying the spectroscopy of water.[45] At the equilibrium distance of the ground state, $R=3.26$ Å, this polarization-type $n \to 3s$ excitation was redshifted to 6.31 eV. The crystal formation caused a redshift of this excitation by 0.7 eV. The electron-transfer-type excitation energy was as large as 12.8 eV at $R=100$ Å, but becomes much smaller to 10.2 eV at the ground-state equilibrium distance. The redshift caused by the crystal formation was as large as 2.6 eV.

Next, we examine the properties of the potential curves. Reflecting the dipole-dipole interaction between the water monomers, the ground state was attractive and had a minimum at 3.26 Å with a depth of about 4.23 eV. The lower excited states were $n \to 3s$ polarization type when R is large, but the nature became a mixed type between polarization and electron-transfer types at a shorter distance of R. Above these states, pure electron-transfer states existed. Since electron transfer is difficult when R is large but becomes easier when R becomes small, the potential curve of the electron-transferred state was stabilized more as R becomes smaller than those of the polarization-dominant states and the ground state. From Table VIII, we see that the polarization state has minima at 3.20 Å with a depth of 4.96 eV. On the other hand, the electron-transfer state has minima at 3.23 Å with a depth of 6.85 eV. The minimum of the electron-transferred state is deeper than that of the polarization state, which is still deeper than that of the ground state. The deepness of the polarization state in comparison with the ground state is partially due to the mixing of the electron-transferred-type excitations to the pure polarization-type ones in a shorter distance of R. The equilibrium interwater distance was very similar among the ground and two types of excited states: the difference was within 0.1 Å. So, the geometrical change is not a useful photo induced property of this crystal. Rather, a merit of this crystal is that both the ground and excited states are stable at around the same geometry, having clear minima on the potential curves, so that for photofunctional devices, we may use other properties that are different between the ground and excited states.

C. H_2CO ring crystal

Finally, we study the H_2CO ring crystal with the giant SAC/SAC-CI method. The SAC/SAC-CI calculation on free formaldehyde[47] may be a good reference. We calculated the ring crystals of the sizes $N=50$, 100, and 500, and we first show the results for $N=50$. The arrangement of the formaldehyde monomer in the ring crystal was shown in Fig. 4(d). It is an alternating arrangement which is advantageous for the dipole-dipole interaction between the monomers like in the H_2O ring crystal. Different from the arrangement in the water crystal, all the H_2CO monomers are in the same environment. The basis set was D95. The selection level in the SAC/SAC-CI calculations was level 2.[12] We included all the MO space as active except for the $1s$ core orbitals of carbon and oxygen. The potential energy curves for the ground state and the $n \to \pi^*$ and $\pi \to \pi^*$ excited states of the ring crystal against the variation of the interformaldehyde distance R were shown in Fig. 7. The potential properties calculated
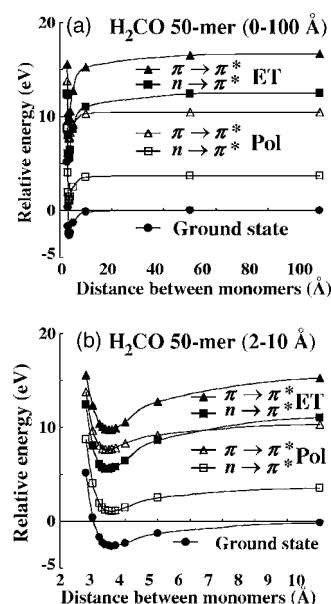

FIG. 7. The potential energy curves of the ground, polarization (Pol)-type, and electron-transfer (ET)-type $n \to \pi^*$ and $\pi \to \pi^*$ excited states of H_2CO 50-mer: (a) 0–100 Å and (b) 2–10 Å.

TABLE IX. Potential properties and vertical excitation energies of the H_2CO 50-mer ring crystal.

| | | | R_e[a] (Å) | ω_e[b] (cm^{-1}) | Depth[c] (eV) | Vertical excitation energy (eV) | | | |
						$R=R_e$[d]	$R=100.0$[d]	Monomer	Expt.[e]
	Ground state		3.59	300	2.663				
Excited states	Pol[f]	$n \to \pi^*$	3.57	304	2.681	3.728	3.746	3.794	4.1
		$\pi \to \pi^*$	3.44	352	2.876	10.383	10.514	10.578	10.7
	ET[g]	$n \to \pi^*$	3.45	397	7.019	8.263	12.526	12.410	
		$\pi \to \pi^*$	3.49	373	6.924	12.487	16.706	16.648	

[a]Equilibrium distance between monomers.
[b]Vibrational frequency.
[c]The depth of potential energy curves.
[d]The distance between monomers.
[e]Reference 47.
[f]Polarization type.
[g]Electron transfer type.

from these potential curves and the vertical excitation energies from the equilibrium distance of the ground state were summarized in Table IX.

The ground state is attractive and has a minimum at $R = 3.59$ Å with a depth of 2.66 eV. In comparison with the water ring crystal, the equilibrium distance is longer and the depth of the potential well is smaller. For H_2CO, four kinds of excited states were examined: polarization and electron transfer $n \to \pi^*$ states and polarization and electron transfer $\pi \to \pi^*$ states. The electron-transfer excited states are due to the excitations to the nearest neighbor monomer, so that their excited states are higher than the polarization type excited states when the distance R is large. The $n \to \pi^*$ polarization state is always the lowest excited state of the H_2CO ring crystal and has a minimum at 3.57 Å with a depth of 2.68 eV: these properties are very similar to those of the ground state. On the other hand, the $n \to \pi^*$ electron-transfer excited state, which is higher than both of the $n \to \pi^*$ and $\pi \to \pi^*$ polarization-type excited states when R is large, becomes lower than the $\pi \to \pi^*$ polarization-type excited state when R becomes small, as seen in Fig. 7. The electron-transfer states are very much stabilized at shorter distances because of the Coulomb attractions and the overlap interactions between the two monomers, so that they have much steeper potential curves than those of the polarization states. This is seen in Table IX from the potential depth value and the ω_e value. The former is 7.02 eV in comparison with 2.68 eV of the polarization states and the latter is $373 - 397$ cm^{-1} in comparison with $304 - 352$ cm^{-1} of the polarization states. The equilibrium distances R_e of the ground and $n \to \pi^*$ polarization states are both at about 3.60 Å, while the equilibrium distances R_e of the other three states, the $\pi \to \pi^*$ polarization state and the two electron-transfer states, have minima at similar shorter distances of $3.44 - 3.49$ Å. Interestingly, the excitations to these excited states make the size of the ring crystal shrink, and the ring crystal will expand again after the relaxation to the lower two states.

Table IX also shows the vertical exitation energies of the ring crystal from the ground state at $R = 100$ Å and at $R = R_e$. It also shows the vertical excitation energies for infinitely separated monomers. The vertical excitation energies

of the two polarization excited states are almost the same, 3.7 and 10.4 eV, independent of the distance R, and they are rather close to the experimental values, 4.1 and 10.7 eV,[48] despite of the crudeness of the basis set. However, the excitation energies of the two electron-transfer excited states are very much dependent on the inter H_2CO distance: at $R = R_e$, 8.26 eV $(n \to \pi^*)$ and 12.49 eV $(\pi \to \pi^*)$, but at $R = 100.0$ Å, 12.53 $(n \to \pi^*)$ and 16.71 eV $(\pi \to \pi^*)$. This is due to the increasing stabilization of the electron-transfer excited states at a shorter distance of R. However, the R_e, ω_e, and depth are almost the same between the two electron-transfer excited states.

We examine the lowest $n \to \pi^*$ polarization state in more detail. For the ring crystal of $N = 50$, there should be 50 similar states corresponding to the single $n \to \pi^*$ excited state of H_2CO. We have calculated all such states at the equilibrium
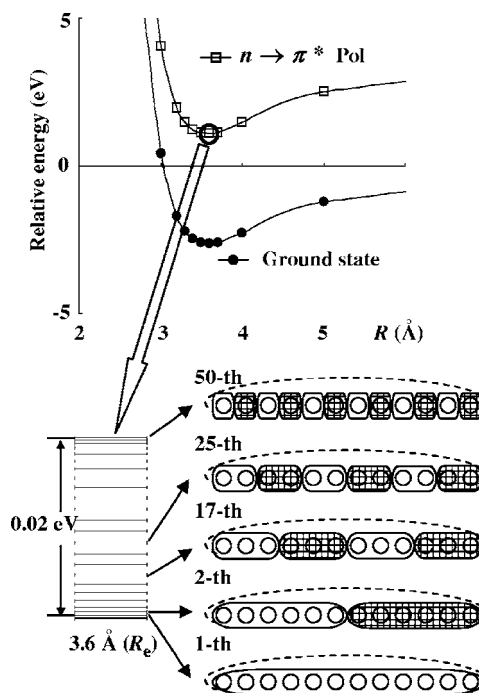

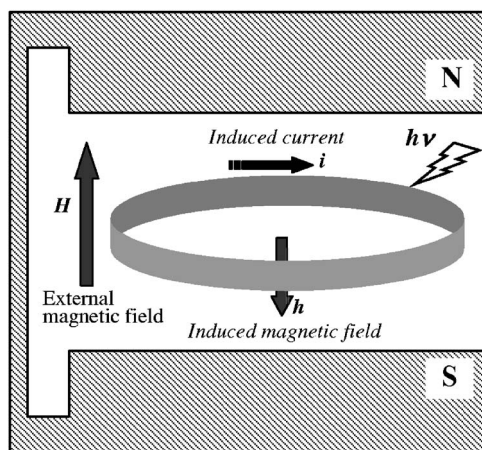FIG. 8. Band structure of the polarization-type $n \to \pi^*$ excited state of H_2CO 50-mer at 3.6 Å.

FIG. 9. Ring crystal of H_2CO in the magnetic field exposed to the light of about 3.7 eV.

distance $R_e = 3.6$ Å of the ground state, and the results are illustrated in Fig. 8. These 50 states form a band spread within only 0.02 eV. The lowest level correspond to the nodeless totally symmetric state, the second lowest one to the state having one node, etc. But since all these states are within only 0.02 eV (0.46 kcal/mol), even a small thermal perturbation is enough to mix up these states and the Wannier local states will be produced. For example, when an external magnetic field is applied in the direction perpendicular to the plane of the ring crystal and the light of about 3.7 eV is irradiated to the crystal, as illustrated in Fig. 9, a ring current (denoted as i) will be induced in the lifetime of the excited state in the direction whose induced magnetic field is opposite to the applied magnetic field. This system may be utilized as a photoswitch or a photosensor. This is an example of the usefulness of the giant molecular systems, in particular, of their excited electronic structures. It gives useful information for molecular design and we hope that the present methodology serves a useful tool for such studies.

Finally, we have applied the present method not only to 50-mer, but also to 100- and 500-mers of the H_2CO ring crystal. As explained before, the formation of the matrix element is quite easy, independent of the size of the crystal, and the computational time increases only at the diagonalization step. We calculated the excitation energy of the crystal at $R = 3.6$ Å, and the result was given in Table X. As expected, the crystal size dependence of the excitation energy is small. Among the four excited states, the polarization-type $\pi \rightarrow \pi^*$ excitation depends mostly on the crystal size. This excitation seems to be affected mostly by the angle between the two

TABLE X. Excitation energies (eV) of H_2CO 50-, 100-, and 500-mer ring crystals.

N[a]	Polarization type		Electron-transfer type	
	$n \rightarrow \pi^*$	$\pi \rightarrow \pi^*$	$n \rightarrow \pi^*$	$\pi \rightarrow \pi^*$
50	3.748	10.422	8.299	12.354
100	3.749	10.503	8.303	12.346
500	3.751	10.593	8.308	12.360

[a]Number of monomers.

H_2CO planes among the calculated four types of excitations. The excitation energies generally increase as the size of the crystal increases: only the electron-transfer-type $\pi \rightarrow \pi^*$ excitation shows a different behavior.

VIII. CONCLUSION

We have extended our SAC/SAC-CI methodology to giant molecular systems. This is the first report on this topic. For dealing with the giant molecular systems in chemical accuracy, the size extensivity for the energy and the size intensivity for the properties are quite important. From this requirement and from chemical reliabilities, we have adopted the SAC/SAC-CI methodology for the ground, excited, ionized, and electron-attached states of molecules. We have formulated here the SAC/SAC-CI method for the giant cyclic molecular crystal composed of the same molecular species, which are probably the simplest model giant system and therefore serve as a milestone for extending the theory to general complex giant molecular systems.

We have first defined the zeroth order reference wave function and orbitals for constructing the SAC/SAC-CI wave function of the giant molecular system. It was defined to be close to the Hartree-Fock wave function of the giant system. We have introduced monomer-localized canonical molecular orbitals (ml-CMO's) as the reference orbitals for constructing the SAC/SAC-CI excitation operators. They allow a monomer canonical-orbital picture even in the study of ring crystals. Since electron correlation is a local phenomena, we have focused on the two neighboring monomers A and B surrounded by some numbers of monomers C from both sides. The rest of the crystal, called D region, was approximately replaced by the electrostatic field exerting on the $CABC$ real system. By doing Hartree-Fock calculations on this system and by unitary transforming the resultant MO's into the ml-CMO's, we obtained our reference orbitals of A and B and used them for constructing our reference wave function ψ_0 of the SAC/SAC-CI calculations. These ml-CMO's extend over the $CABC$ region. The energy of this reference wave function ψ_0 was calculated and used as E_0 of the succeeding SAC/SAC-CI calculations. The atomic orbital integrals were transformed into the MO integrals with the use of the ml-CMO's of AB in $CABC$. These MO integrals are all that are necessary for the succeeding SAC/SAC-CI calculations.

The singles and doubles approximation of the SAC/SAC-CI formulation was adopted in this report, and only the excitations within each monomer (polarization) and to the nearest neighbor monomer (electron transfer) were included. The excitations simultaneous to the different nearest neighbor monomers were not included in the present calculations. The perturbation selection of the linked operators was done as in the standard SAC/SAC-CI code in GAUSSIAN 03. We have included almost all the important unlinked terms that arise from the selected linked operators, except for some higher-order operators of the single excitation SAC operators. The unlinked terms are very important not only for describing the higher-order electron correlation effects and the electron correlations transferred to the excited states, but

also for keeping the size extensivity and the size intensivity of the calculated energies and properties. The calculations were done with the new direct algorithm recently developed also for the standard SAC/SAC-CI calculations. Because of the simplicity of the cyclic ring crystals composed of the same molecular species, the computations were much simpler and faster than the standard method in GAUSSIAN 03.

We have examined our theory by doing some test calculations and model calculations. The size extensivity of the energy and the size intensivity of the excitation energy were confirmed in the calculated results of the present giant SAC/SAC-CI method, allowing chemical arguments even for giant molecular systems. We think these properties are very important for the theory of giant molecular systems. The effectiveness of the present method over the conventional standard method for large molecular crystals was confirmed. We have applied the present method to the ground state and the polarization-type and electron-transfer-type excited states of some realistic model systems: C_2H_4 ring crystal, H_2O ring crystal, and H_2CO ring crystal. We have studied the potential energy curves of the ground and excited states as functions of the intermonomer distances of the crystal. Some interesting observations on the natures of the ground state, the polarization-type excited states, and the electron-transfer-type excited states were reported. Generally speaking, Coulomb interactions between crystal monomers are important for the ground-state potential curve, the properties of the polarization-type excited states are rather independent of the intermonomer distances, while those of the electron-transfer states are strongly dependent on the intermonomer distances: the intermonomer attractive interactions increase as the distance becomes shorter. The present method seems to have much potentiality as a useful method for doing molecular design and molecular engineering of molecular crystals.

For example, for the H_2CO ring crystal, a possible molecular design of photoswitch or photosensor was explained. Actually, mesoscopic and nanoscopic rings have potential applications to molecular circuit or devices, and the electromagnetic and photophysical properties of ringlike materials have been studied in some detail.[49] Further, the ring crystal is the simplest model of clusters consisting of a finite number of molecules, and the molecular conformations in simple clusters have been studied.[50] In the previous studies, model particles were used as the elements of the clusters, but in this study, realistic molecules were used as the elements of the ring.

We plan to extend the present methodology to three-dimensional crystals, polymers, and biological systems and such extensions are currently in progress. For three-dimensional cubic molecular crystals, one monomer is surrounded by six nearest neighbor monomers, which may consist of the *A* and *B* regions. The *C* region may include one larger shell, at least. The infinite nature of the system may be taken into account by including periodic boundary conditions in the calculational scheme. For polymers and most biological systems, we have to cut some chemical bonds in a manner that will not affect much the final results. Anyway, the local nature of correlations would serve to simplify the computational algorithms. The good accuracy of the present results serves as the basis in formulating such extensions.

Finally, we note that the energy alone of the giant molecular crystals is rather easily calculated by using the fact that the direct *N*-body interaction energy should converge to zero. This convergence usually occurs at a relatively small tractable size, so that we can calculate all the direct *N*-body interaction energies. Using them we can in principle calculate the energy of arbitrary large molecular crystals. This is true not only at the Hartree-Fock level, but also at the correlation levels. However, such method is valid only for the ground state, and further, it does not give the corresponding wave function. So, such treatment is not interesting as a chemical theory.

[1] H. Nakatsuji, Bull. Chem. Soc. Jpn. **78**, 1705 (2005).
[2] P. A. M. Dirac, Proc. R. Soc. London, Ser. A **123**, 714 (1929).
[3] H. Nakatsuji, J. Chem. Phys. **113**, 2949 (2000); H. Nakatsuji and E. R. Davidson, *ibid.* **115**, 2000 (2001); H. Nakatsuji and M. Ehara, *ibid.* **117**, 9 (2002); **122**, 194108 (2005).
[4] H. Nakatsuji, Phys. Rev. Lett. **93**, 030403 (2004); Phys. Rev. A **72**, 062110 (2005); Y. Kurokawa, H. Nakashima, and H. Nakatsuji, *ibid.* **72**, 062502 (2005); H. Nakatsuji and H. Nakashima, Phys. Rev. Lett. **95**, 050407 (2005).
[5] P. W. Atkins, *Physical Chemistry*, 4th ed. (Oxford University Press, Oxford, 1990), p. 30.
[6] E. Kohen, R. Santus, and J. G. Hirschberg, *Photo Biology* (Academic, New York, 1995).
[7] *The Photosynthetic Reaction Center*, edited by J. Deisenhofer and J. R. Norris (Academic, New York, 1993), Vols. 1 and 2.
[8] H. Kolb, E. Fernandez, and R. Nelson, "Web Vision," John Moran Eye Center, University of Utah (http://webvision.med.utah.edu/).
[9] G. Ashkanazi, R. Kosloff, and M. A. Ratner, J. Am. Chem. Soc. **121**, 3386 (1999).
[10] H. Nakatsuji and K. Hirao, Chem. Phys. Lett. **47**, 569 (1977); J. Chem. Phys. **68**, 2053 (1978).
[11] H. Nakatsuji, Chem. Phys. Lett. **59**, 362 (1978); **67**, 329 (1979); **177**, 331 (1991); H. Nakatsuji and M. Ehara, J. Chem. Phys. **98**, 7179 (1993).
[12] SAC-CI home page, http://www.sbchem.kyoto-u.ac.jp/nakatsuji-lab/sacci.html
[13] H. Nakatsuji, in *Computational Chemistry: Reviews of Current Trends*, edited by J. Leszczynski (World Scientific, Singapore, 1997), Vol. 2, pp. 62–124; M. Ehara, J. Hasegawa, and H. Nakatsuji, *Theory and Applications of Computational Chemistry, The First* 40 Years, edited by C. E. Dykstra, G. Frenking, K. S. Kim, and G. E. Scuseria (Elsevier, Oxford, 2005), Chap. 39, pp. 1099–1141; M. Ehara, M. Ishida, K. Toyota, and H. Nakatsuji, in *Reviews in Modern Quantum Chemistry* (A tribute to Professor Robert G. Parr), edited by K. D. Sen (World Scientific, Singapore, 2003), pp. 293–319.
[14] M. J. Frisch, G. W. Trucks, H. B. Schlegel *et al.*, GAUSSIAN 03, Gaussian, Inc., Pittsburgh, PA, 2003.
[15] T. Nakajima and H. Nakatsuji, Chem. Phys. Lett. **280**, 79 (1997); Chem. Phys. **242**, 177 (1999); M. Ishida, K. Toyoda, M. Ehara, and H. Nakatsuji, Chem. Phys. Lett. **347**, 493 (2001); **350**, 351 (2001); K. Toyoda, M. Ehara, and H. Nakatsuji, Chem. Phys. Lett. **356**, 1 (2002); K. Toyota, M. Ishida, M. Ehara, M. J. Frisch, and H. Nakatsuji, *ibid.* **367**, 730 (2003); M. Ishida, K. Toyota, M. Ehara, M. J. Frisch, and H. Nakatsuji, J. Chem. Phys. **120**, 2593 (2004).
[16] K. Ueda, M. Hoshino, T. Tanaka *et al.*, Phys. Rev. Lett. **94**, 243004 (2005); M. Ehara, H. Nakatsuji, M. Matsumoto *et al.*, J. Chem. Phys. **124**, 124311 (2006); R. Sankari, M. Ehara, H. Nakatsuji, A. De Fanis, H. Aksela, S. L. Sorensen, M. N. Piancastelli, E. Kukk, and K. Ueda, Chem. Phys. Lett. **422**, 51 (2006); M. Ehara, K. Kuramoto, H. Nakatsuji, M. Hoshino, T. Tanaka, M. Kitajima, H. Tanaka, A. De Panis, Y. Tamenori,

and K. Ueda, J. Chem. Phys. **125**, 114304 (2006).

[17] J. Wan, J. Meller, M. Hada, M. Ehara, and H. Nakatsuji, J. Chem. Phys. **113**, 7853 (2000); M. Ehara, M. Ishida, and H. Nakatsuji, *ibid.* **114**, 8990 (2001); **117**, 3248 (2002); M. Ishida, K. Toyota, M. Ehara, H. Nakatsuji, and M. J. Frisch, *ibid.* **120**, 2593 (2004); M. Ehara, Y. Ohtsuka, H. Nakatsuji, M. Takahashi, and Y. Udagawa, *ibid.* **122**, 234319 (2005); T. Nakajima, S. Hane, and K. Hirao, *ibid.* **124**, 224307 (2006).

[18] H. Nakatsuji, J. Hasegawa, and K. Ohkawa, Chem. Phys. Lett. **296**, 499 (1998); J. Hasegawa, K. Ohkawa, and H. Nakatsuji, J. Phys. Chem. B **102**, 10410 (1998); J. Hasegawa and H. Nakatsuji, J. Phys. Chem. B **102**, 10420 (1998); J. Hasegawa and H. Nakatsuji, Chem. Lett. **34**, 1242 (2005).

[19] K. Fujimoto, J. Hasegawa, S. Hayashi, S. Kato, and H. Nakatsuji, Chem. Phys. Lett. **414**, 239 (2005).

[20] A. Imamura, Y. Aoki, and K. Maekawa, J. Chem. Phys. **95**, 5419 (1991); A. Imamura, Y. Aoki, K. Nishimoto, Y. Kurihara, and A. Nagao, Int. J. Quantum Chem. **52**, 309 (1994).

[21] Y. Aoki, S. Suhai, and A. Imamura, J. Chem. Phys. **101**, 10808 (1994); M. Mitani and A. Imamura, *ibid.* **103**, 663 (1995); M. Mitani, Y. Aoki, and A. Imamura, Int. J. Quantum Chem. **64**, 301 (1997); Y. Kurihara, Y. Aoki, and A. Imamura, J. Chem. Phys. **107**, 3569 (1997); F. L. Gu, Y. Aoki, J. Korchowiec, A. Imamura, and B. Kirtman, *ibid.* **121**, 10385 (2004); J. Korchowiec, F. L. Gu, and Y. Aoki, Int. J. Quantum Chem. **105**, 875 (2005).

[22] W. Förner, R. Knab, J. Cizek, and J. Ladik, J. Chem. Phys. **106**, 10248 (1997).

[23] K. Kitaura, T. Sawai, T. Asada, T. Nakano, and M. Uebayashi, Chem. Phys. Lett. **312**, 319 (1999); K. Kitaura, E. Ikeo, T. Asada, T. Nakano, and M. Uebayashi, *ibid.* **313**, 701 (1999); D. G. Fedorov, R. M. Olson, K. Kitaura, M. S. Gordon, and S. Koseki, J. Comput. Chem. **25**, 872 (2004); D. G. Fedorov and K. Kitaura, J. Chem. Phys. **120**, 6832 (2004).

[24] F. Sato, Y. Shigemitsu, I. Okazaki, S. Yahiro, M. Fukue, S. Kozuru, and H. Kashiwagi, Int. J. Quantum Chem. **63**, 245 (1997); F. Sato, T. Yoshihiro, M. Era, and H. Kashiwagi, Chem. Phys. Lett. **341**, 645 (2001).

[25] S. Goedecker, Rev. Mod. Phys. **71**, 1085 (1999).

[26] S. Saebo and P. Pulay, Annu. Rev. Phys. Chem. **44**, 213 (1993).

[27] W. Yang, Phys. Rev. Lett. **66**, 1438 (1991); Phys. Rev. A **44**, 7823 (1991); W. Yang and T.-S. Lee, J. Chem. Phys. **163**, 5674 (1995).

[28] G. E. Scuseria, J. Phys. Chem. A **103**, 4782 (1999); K. N. Kudin and G. E. Scuseria, Phys. Rev. B **61**, 16440 (2000).

[29] C. Hampel and H.-J. Werner, J. Chem. Phys. **104**, 6286 (1996); M. Schütz and H.-J. Werner, Chem. Phys. Lett. **318**, 370 (2000); J. Chem. Phys. **114**, 661 (2001).

[30] M. Schütz, G. Hetzer, and H.-J. Werner, J. Chem. Phys. **111**, 5691 (1999); G. Hetzer, M. Schütz, H. Stoll, and H.-J. Werner, *ibid.* **113**, 9443 (2000); C. Pisani, M. Busso, G. Capecchi, S. Casassa, R. Dovesi, L. Maschio, C. Zicovich-Wilson, and M. Schütz, *ibid.* **122**, 094113 (2005); H.-J. Werner and F. R. Manby, *ibid.* **124**, 054114 (2006); F. R. Manby, H.-J. Werner, T. B. Adler, and A. J. May, *ibid.* **124**, 094103 (2006).

[31] Y. H. Shao, C. A. White, and M. Head-Gordon, J. Chem. Phys. **114**, 6572 (2001); C. Saravanan, Y. Shao, R. Baer, P. N. Ross, and M. Head-Gordon, J. Comput. Chem. **24**, 618 (2003); W. Z. Liang, C. Saravanan, Y. H. Shao, R. Baer, A. T. Bell, and M. Head-Gordon, J. Chem. Phys. **119**, 4117 (2003); Y. Jung, A. Sodt, P. M. W. Gill, and M. Head-Gordon, Proc. Natl. Acad. Sci. U.S.A. **102**, 6692 (2005); R. A. DiStasio, Y. S. Jung, and M. Head-Gordon, J. Chem. Theory Comput. **1**, 862 (2005).

[32] T. Nakajima and K. Hirao, J. Chem. Phys. **124**, 184108 (2006); Y. Kurashige, T. Nakajima, and K. Hirao, Chem. Phys. Lett. **417**, 241 (2006); T. Nakajima and K. Hirao, *ibid.* **427**, 225 (2006).

[33] For example, M. Pope and C. E. Swenberg, *Electronic Processes in Organic Crystals and Polymers*, 2nd ed. (Oxford University Press, New York, 1999).

[34] K. Fukui, *Theory of Orientation and Stereoselection* (Springer-Verlag, Berlin, 1995); Acc. Chem. Res. **4**, 57 (1971).

[35] R. B. Woodward and R. Hoffmann, Angew. Chem., Int. Ed. Engl. **8**, 781 (1969).

[36] O. Sinanoglu, Proc. Natl. Acad. Sci. U.S.A. **47**, 1217 (1961).

[37] D. J. Thouless, Nucl. Phys. **21**, 225 (1960).

[38] S. F. Boys, Rev. Mod. Phys. **32**, 306 (1960).

[39] J. Pipek and P. G. Mezey, J. Chem. Phys. **90**, 4916 (1989).

[40] R. Fukuda and H. Nakatsuji (unpublished).

[41] C. M. Reeves, Commun. ACM **9**, 276 (1966); B. T. Sutcliffe, J. Chem. Phys. **45**, 235 (1966).

[42] K. Hirao and H. Nakatsuji, J. Comput. Phys. **45**, 246 (1982).

[43] H. Nakatsuji, J. Chem. Phys. **80**, 3703 (1984); C. C. Ballard, M. Hada, and H. Nakatsuji, Bull. Chem. Soc. Jpn. **69**, 1901 (1996); J. Hasegawa, M. Ehara, and H. Nakatsuji, Chem. Phys. **230**, 23 (1998).

[44] T. H. Dunning, Jr. and P. J. Hay, in *Modern Theoretical Chemistry*, edited by H. F. Schaefer III (Plenum, New York, 1977), Vol. 3, p. 1.

[45] H. Nakatsuji and K. Hirao, Int. J. Quantum Chem. **20**, 1301 (1981); K. Hirao and H. Nakatsuji, Chem. Phys. Lett. **79**, 292 (1981).

[46] N. W. Winter, W. A. Goddard III, and F. W. Bobrowicz, J. Chem. Phys. **62**, 4325 (1975).

[47] H. Nakatsuji, K. Ohta, and K. Hirao, J. Chem. Phys. **75**, 2952 (1981).

[48] S. R. Langhoff and E. R. Davidson, J. Chem. Phys. **64**, 4699 (1976).

[49] A. Matos-Abiague and J. Berakdar, Phys. Rev. Lett. **94**, 166801 (2005).

[50] I. V. Schweigert, V. A. Schweigert, and F. M. Peeters, Phys. Rev. B **54**, 10827 (1996).